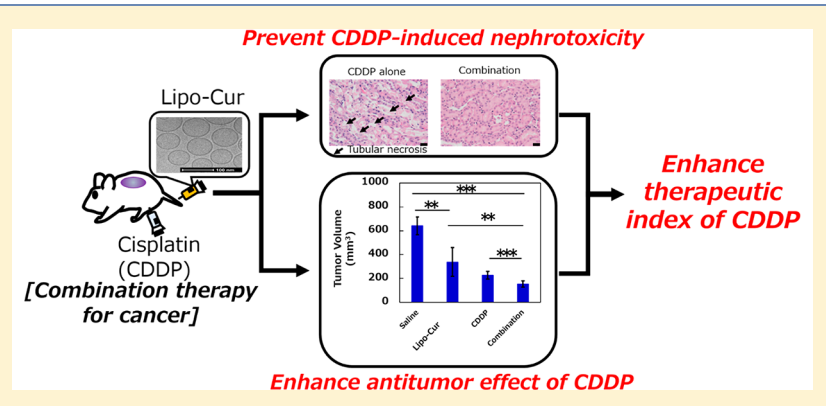
Cite This: Mol. Pharmaceutics 2019, 16, 3957-3967

Robust Microfluidic Technology and New Lipid Composition for Fabrication of Curcumin-Loaded Liposomes: Effect on the **Anticancer Activity and Safety of Cisplatin**

Nobuhito Hamano,[†] Roland Böttger,[†] Suen Ern Lee,[†] Yang Yang,[†] Jayesh A. Kulkarni,[‡] Shell Ip,[#] Pieter R. Cullis, to and Shyh-Dar Li*, to

^{*}Precision NanoSystems Inc, Vancouver, British Columbia V6P 6T7, Canada



ABSTRACT: Curcumin exhibits potent anticancer activity via various mechanisms, but its in vivo efficacy has been hampered by poor solubility. Nanotechnology has been employed to deliver curcumin, but most of the reported systems suffered from low drug loading capacity and poor stability. Here, we report the development and optimization of a liposomal formulation for curcumin (Lipo-Cur) using an automated microfluidic technology. Lipo-Cur exhibited a mean diameter of 120 nm with a low polydispersity index (<0.2) and superior loading capacity (17 wt %) compared to other reported liposomal systems. Lipo-Cur increased the water solubility of curcumin by 700-fold, leading to 8-20-fold increased systemic exposure compared to the standard curcumin suspension formulation. When coadministered with cisplatin to tumor-bearing mice, Lipo-Cur augmented the antitumor efficacy of cisplatin in multiple mouse tumor models and decreased the nephrotoxicity. This is the first report demonstrating the dual effects of curcumin enabled by a nanoformulation in enhancing the efficacy and reducing the toxicity of a chemo-drug in animal models under a single and low dose administration.

KEYWORDS: lipid nanoparticles, curcumin, cisplatin, enhanced efficacy and reduced toxicity, microfluidics

1. INTRODUCTION

Downloaded via UNIV OF BRITISH COLUMBIA on March 16, 2020 at 20:01:51 (UTC). See https://pubs.acs.org/sharingguidelines for options on how to legitimately share published articles.

Curcumin belonging to the polyphenols superfamily is the active component of turmeric, and it has been shown to possess a wide range of pharmacological activities including anti-inflammatory, 1,2 anticancer, antioxidant, 4,5 wound healing,6 and antimicrobial effects.7 Curcumin is classed as safe for human use by the U.S. Food and Drug Administration⁸ and is widely consumed as a condiment without any significant side effects. For the above reasons, many researchers have studied curcumin as an anticancer drug, a chemo-sensitizing agent, or a chemo-protecting agent. $^{9-14}$ However, these different effects of curcumin were mostly demonstrated with various dosages and dosing regimens, 10-12,15 and a high dose, frequent administrations, and pretreatment were required (>100 mg/kg, daily doses for 5 days) for significant activities, 15 likely due to its low bioavailability caused by poor aqueous solubility (0.4 μ g/ $mL).^{16}$

To overcome the solubility problem and increase the systemic exposure, various nanotechnology-based delivery systems have been developed for curcumin such as liposomes, polymer-based micelles, and nanoemulsions. 17-22 Among these systems, liposomes are attractive due to their high biocompatibility and established safety profiles. However, the loading capacity of the reported liposomes or nanoemulsions for hydrophobic compounds like curcumin is typically <5 wt %. 17-19 Liposomes are generally produced with the thin-film hydration and membrane extrusion method. Although this method has been standardized, its tedious nature sometimes leads to inconsistent quality, especially in larger scales.

Received: May 27, 2019 Revised: August 2, 2019 Accepted: August 5, 2019 Published: August 5, 2019



[†]Faculty of Pharmaceutical Sciences and [‡]Department of Biochemistry and Molecular Biology, University of British Columbia, Vancouver, British Columbia V6T 1Z3, Canada

Recently, microfluidic techniques have been introduced to fabricate liposomes in an automated fashion. ^{23–27} In general, lipids dissolved in ethanol are rapidly mixed with an aqueous phase in a microfluidic chamber, promoting their self-assembly into liposomes. The mixing rate, solvent ratio, and reaction temperature can be fine-tuned to obtain optimal results. This automated process allows efficient manufacturing of liposomes in a well-controlled manner.

In this study, we aimed to develop and optimize a new liposomal formulation to increase the loading capacity for curcumin using an automated microfluidic technology. We examined multiple factors that could lead to the production of different liposomal curcumins including lipid composition, method of fabrication, microfluidic mixing speed, and solvent ratio. We then characterized the optimal formulation and compared it with the reported ones. To demonstrate the potential utility of this liposomal curcumin, we then examined its antitumor efficacy and effect of reducing nephrotoxicity when combined with cisplatin in animal models. To the best of our knowledge, this is the first report investigating both formulation and manufacturing techniques to increase liposomal loading capacity for curcumin as well as examining the dual effects of curcumin enabled by nanotechnology in augmenting the efficacy and reducing the side effect of an anticancer drug in animal study under a single and low dose administration. This report also provides the first example of liposomal curcumin produced by microfluidics by the time the manuscript was composed.

2. MATERIALS AND METHODS

- **2.1. Materials.** 1,2-Dimyristoyl-sn-glycero-3-phosphocholine (DMPC), 1,2-dipalmitoyl-sn-glycero-3-phosphocholine (DPPC), and 1,2-distearoyl-sn-glycero-3-phosphocholine (DSPC) were purchased from Avanti Polar Lipids, Inc. (Alabaster, AL). Curcumin was acquired from Alfa Aesar (Ward Hill, MA). Tween 80 was obtained from Sigma-Aldrich (St. Louis, MO).
- **2.2. Cells and Animals.** EMT6, a murine breast cancer cell line, and B16F10, a murine melanoma cell line, were obtained from the American Type Culture Collection (ATCC). The cells were maintained in Dulbecco's modified Eagle medium (DMEM) supplemented with 10% fetal bovine serum, penicillin (100 U/mL), and streptomycin (100 μ g/mL) (Hyclone). BALB/c mice and C57BL/6 mice (6–9 weeks, female) were purchased from Jackson Laboratories (Bar Harbour, ME). All protocols were approved by the Animal Care Committee of the University of British Columbia (Vancouver, BC, Canada).
- 2.3. Preparation of Liposomal Curcumin (Lipo-Cur). Lipo-Cur was prepared by microfluidics using a NanoAssemblr Benchtop (Precision Nanosystems Inc., Vancouver, BC, Canada) equipped with a Staggered Herringbone Micromixer. DMPC (4.53 mg) and curcumin (1 mg) were dissolved in 0.5 mL of ethanol. This organic phase was then injected into the right inlet of the micromixer to mix with the aqueous phase (0.182 mg Tween 80/ml PBS) injected from the left inlet at a total flow rate (TFR) of 17 mL/min and a volumetric flow rate ratio (FRR) of 1:5 (organic/aqueous). Under these conditions, the drug-to-total lipid ratio (D/L) was 1:5 (wt) and DMPC/Tween 80 ratio was 95:5 (mol). The resulting dispersions collected from the outlet stream were immediately incubated at 4 °C for 1 h for equilibrium. The product was then dialyzed

(MWCO 10 kDa) against PBS at room temperature for overnight for purification.

Alternatively, Lipo-Cur was prepared using the thin-film hydration method. Briefly, 4.54 mg of DMPC, 0.46 mg of Tween 80, and 1 mg of curcumin were dissolved in 1–3 mL of ethanol, which was then removed by rotary evaporator to form a thin lipid film. The film was then hydrated with 1 mL of PBS at 37 °C, followed by membrane extrusion (pore size 100 nm for 20 times). Lipo-Cur was stored at 4 °C until analysis.

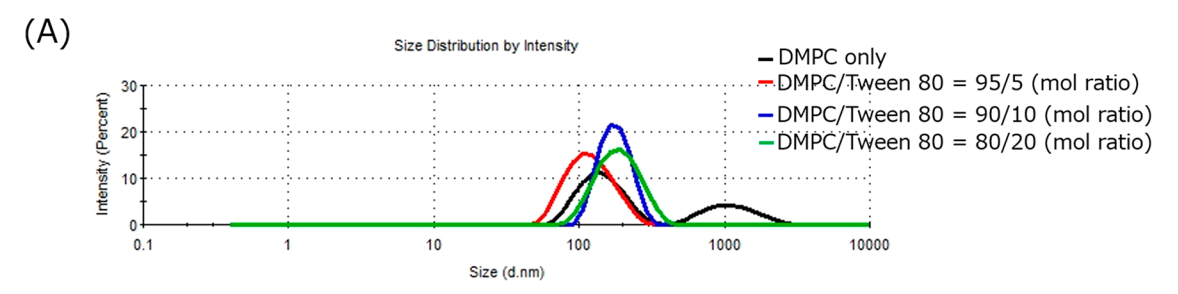
- **2.4.** Characterization of Lipo-Cur. 2.4.1. Size. Particle size and polydispersity index (PDI) of liposomes were measured by a particle analyzer (Zetasizer Nano-ZS, Malvern Instruments Ltd., Malvern, UK).
- 2.4.2. Curcumin Dose Recovery and Estimated D/L and Loading Capacity. After dialysis, Lipo-Cur was collected and weighed, and the final volume was calculated (density \sim 1). Lipo-Cur was diluted with DMSO and analyzed for curcumin concentration using a fluorescence microplate reader (excitation, 485 nm; emission, 535 nm; Hidex Sense, Hidex, Turku, Finland). The recovered amount of curcumin = measured concentration of Lipo-Cur \times total volume. Curcumin dose recovery (%) = Recovered curcumin (mg)/initial input of curcumin (mg) \times 100. Estimated D/L (wt) = Initial input D/L \times curcumin dose recovery (%). Estimated loading capacity is calculated using the following formula:

Estimated loading capacity (%)

- = Recovered amount of curcumin
 - \div (Recovered amount of curcumin + initial input

amount of total lipids) \times 100

- 2.4.3. Cryo-Transmission Electron Microscopy (Cryo-TEM). Cryo-TEM was performed as previously described.²⁸ Briefly, Lipo-Cur was concentrated to a final concentration of 15-25 mg/mL of total lipid. Approximately, $3-5 \mu L$ of Lipo-Cur was added onto a glow-discharged copper grid and plunge-frozen using a FEI Mark IV Vitrobot (FEI, Hillsboro, OR) to generate vitreous ice. The grid was stored in liquid nitrogen until imaged. Prior to imaging, the grid was transferred using a Gatan 70° cryo-tilt transfer system pre-equilibrated at −180 °C and then inserted into an FEI LaB6 G2 transmission electron microscope (FEI, Hillsboro, OR) operated at 200 keV under low-dose conditions. A bottom-mount FEI Eagle 4K CCD camera was used to capture all images. The sample was imaged at a 55 000× magnification with a nominal under focus of 1−2 µm to enhance the contrast. Sample preparation and imaging were performed at the UBC Bioimaging Facility (Vancouver, BC, Canada).
- 2.4.4. Drug Release in Serum. Relative drug release was conducted using the fluorescence dequenching method, as described before. This well-established method to study liposomal fluorophores, such as doxorubicin, utilizes the liposome-encapsulated curcumin as a self-dequenching material to detect the drug in serum following release from the liposome. Lipo-Cur was diluted with sterile PBS to adjust the Cur concentration to 90 μ g/mL, then mixed 1:1 (v/v) with FBS (fetal bovine serum, Gibco Laboratories, Gaithersburg, MD) and incubated at 37 °C. After 10 and 20 min as well as 1, 2, 4, and 24 h, a sample (10 μ L) was collected and diluted with PBS (155 μ L). This mixture (150 μ L) was transferred to a 96-well plate, and immediately the fluorescence was detected using a microplate reader (excitation, 485 nm; emission, 535



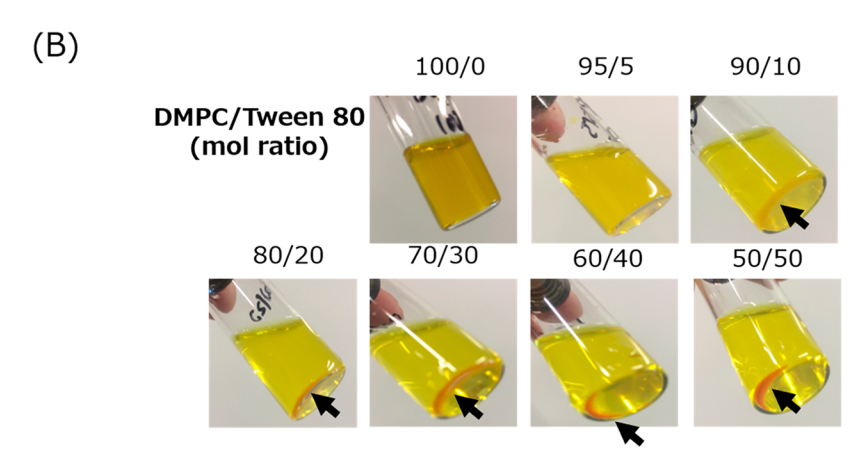


Figure 1. Size distribution profiles (A) and appearance after 1 day storage (B) of different liposomal curcumin formulations. Arrow indicates precipitations.

nm). The drug release (%) at each time point was calculated using the equation below, where F_t denotes the fluorescence at the selected time point, F_0 is the fluorescence at time 0, and F_{100} is the fluorescence of sample (10 μ L) mixed with aqueous Triton-X 100 (15 μ L, 10%, w/w) and then diluated with PBS (140 μ L):

Drug release (%) =
$$(F_t - F_0)/(F_{100} - F_0) \times 100$$

- **2.5. Animal Studies.** Female BALB/c and C57/BL6 mice (18–20 g) were purchased from The Jackson Laboratory (Bar Harbor, ME). All in vivo studies were conducted in accordance with the established experimental protocols approved by the Animal Care Committee of the University of British Columbia (Vancouver, BC, Canada).
- 2.6. Pharmacokinetic (PK) Study of Curcumin Formulations. Female C57BL6 mice (7-8 weeks old) received an i.v. or oral dose of Lipo-Cur or a curcumin suspension (in 0.25% carboxymethylcellulose) at 20 mg/kg. The widely used curcumin suspension formulation was adopted from the literature 15,30 as a reference to compare the PK with our innovative Lipo-Cur. Plasma (30 μ L) was collected from the mice at 1, 15, 30, 60, and 180 min, then mixed with 90 μ L of acetonitrile, and centrifuged at 5000 rpm at 4 °C for 5 min. Fluorescence of the supernatant was measured by using a plate reader (excitation, 485 nm; emission, 535 nm), and the fluorescence intensity was compared to a standard curve (0-10 μ g/mL) to obtain the curcumin concentration. PK parameters of Lipo-Cur including T_{max} C_{max} and elimination half-life were obtained by fitting the data with the Phoenix WinNonlin software (Princeton, NJ). Area under the curve (AUC) was calculated using the trapezoidal rule.
- **2.7.** Efficacy against Tumor Models of EMT6 and B16F10. EMT6 or B16F10 cells (2×10^5 cells) were s.c. inoculated into the shaved right lateral flank of female BALB/c or C57BL6 mice, respectively. When tumors reached the size of 50 mm³ (B16F10) or 150 mm³ (EMT6), the mice were treated with either saline (i.p.), cisplatin (CDDP) alone (15 mg CDDP/kg, i.p.), Lipo-Cur alone (20 mg curcumin/kg, i.v.) or a combination of CDDP and Lipo-Cur. For the combination, CDDP (15 mg CDDP/kg, i.p.) was administered first, immediately followed by i.v. Lipo-Cur alone (20 mg curcumin/kg). Tumor size was monitored using a caliper.
- 2.8. Protective Effect against CDDP-Induced Nephrotoxicity. BALB/c mice were treated with either saline (i.p.), CDDP alone (15 mg CDDP/kg, i.p.), Lipo-Cur alone (20 mg curcumin/kg, i.v.), or CDDP + Lipo-Cur. Three days later, serum was sampled from the mice, followed by animal euthanasia and kidney collection. The dose-limiting toxicity of CDDP is nephrotoxicity. Therefore, to examine the kidney toxicity from the treatments, the serum samples were analyzed for blood urea nitrogen (BUN) (UBC Centre for Comparative Medicine), and the kidney samples were fixed in 10% formalin, followed by paraffin tissue section and hematoxylin/eosin staining for histological analysis. The tissue histology was analyzed by a certified animal pathologist at the UBC Centre for Comparative Medicine.
- **2.9. Statistical Analysis.** All data are expressed as mean \pm SD. Statistical analysis was conducted with the two-tailed unpaired t test for two group comparison or one-way ANOVA, followed by the Tukey multiple comparison tests by GraphPad Prism (for three or more groups). A difference with p < 0.05 was considered to be statistically significant.

3. RESULTS AND DISCUSSION

3.1. Optimization of Liposomal Curcumin. *3.1.1. DMPC/Tween 80 Ratio.* To initiate the formulation development process, we fixed the microfluidic conditions (total flow rate = 17 mL/min; organic/aqueous phase ratio = 1:5) and focused on investigating the optimal lipid composition. We first attempted to formulate curcumin in DMPC only liposomes, but multiple-peak distribution of size was found (Figure 1A) with a large PDI of 0.276 (Table 1).

Table 1. Size and PDI of Various Liposomal Curcumin Formulations^a

lipid ratio [DMPC/Tween 80 (mol)]	size (nm)	PDI
100:0	148.4 ± 31.2	0.276 ± 0.125
95:5	117.1 ± 4.57	0.120 ± 0.005
90:10	154.6 ± 23.0	0.073 ± 0.025
80:20	168.8 ± 5.26	0.166 ± 0.045
70:30	264.2 ± 154.1	0.334 ± 0.148
50:50	349.5 ± 168.8	0.465 ± 0.110
^a Data = mean \pm S.D ($n = 3$).		

Including 5–20 mol % Tween 80 in the lipid formulation produced particles with single-peak size distribution and a narrow PDI (<0.2). Our data also showed a trend of increasing particle size with increasing Tween 80 content: liposomal formulations containing 5, 20, and 50 mol % of Tween 80 exhibited an increase of ~120 nm, ~170 nm, and ~350 nm in particle size, respectively. After 1 day storage at 4 °C, formulations containing 10 mol % or more Tween 80 displayed yellow precipitates (Figure 1B), which suggested instability. The 95:5 formulation, on the other hand, remained stable without any change in particle size and PDI after 3

weeks of storage. Tween 80 is a water-soluble surfactant and is composed of a linear acyl chain as the hydrophobic component and three blocks of PEG chains connected through a tetrahydrofuran group as the hydrophilic head. When presents in a low quantity, Tween 80 intercalates into the lipid bilayer, granting PEGylation to the liposomal surface to reduce fusion of liposomes and improve the stability. However, Tween 80 as a detergent disrupts the lipid bilayer when present in a high concentration. Our results showed that 5 mol % of Tween 80 appeared to be optimal. This observation was consistent with the report from Israelachvili et al., 31,32 who introduced terms of "vesicle solubilization" and "packing parameter" to explain the mechanism how a surfactant could solubilize phospholipids. In short, the structures of a surfactant and a phospholipid are different, and thus, their packing parameters are different (<0.33 and \sim 1, respectively). The differences drive their packing in water either into a micellar or a bilayer conformation. When these two molecules are mixed, the overall packing parameter is decreased, favoring the formation of a micellar structure. 33,34 Therefore, at a high ratio of Tween 80/PC, the resulting vesicles could be in the micellar form that displays a low capacity for curcumin loading. A ratio between PC and Tween 80 at 95:5 (mol) was selected for the following studies.

3.1.2. Acyl Chain Length of Phospholipid. At a fixed PC/Tween 80 ratio of 95:5 (mol) and a fixed initial D/L ratio of 1:5 (wt), we then examined how the acyl chain length of PC affected the resulting liposomal formulation for curcumin. Three PCs containing different acyl chain lengths were used and compared including DMPC (C14), DPPC (C16), and DSPC (C18). As shown in Figure 2A, curcumin formulations prepared with DPPC and DSPC displayed significant aggregation with a large diameter (>3000 nm) and PDI (>0.8), and only the DMPC formulation could incorporate

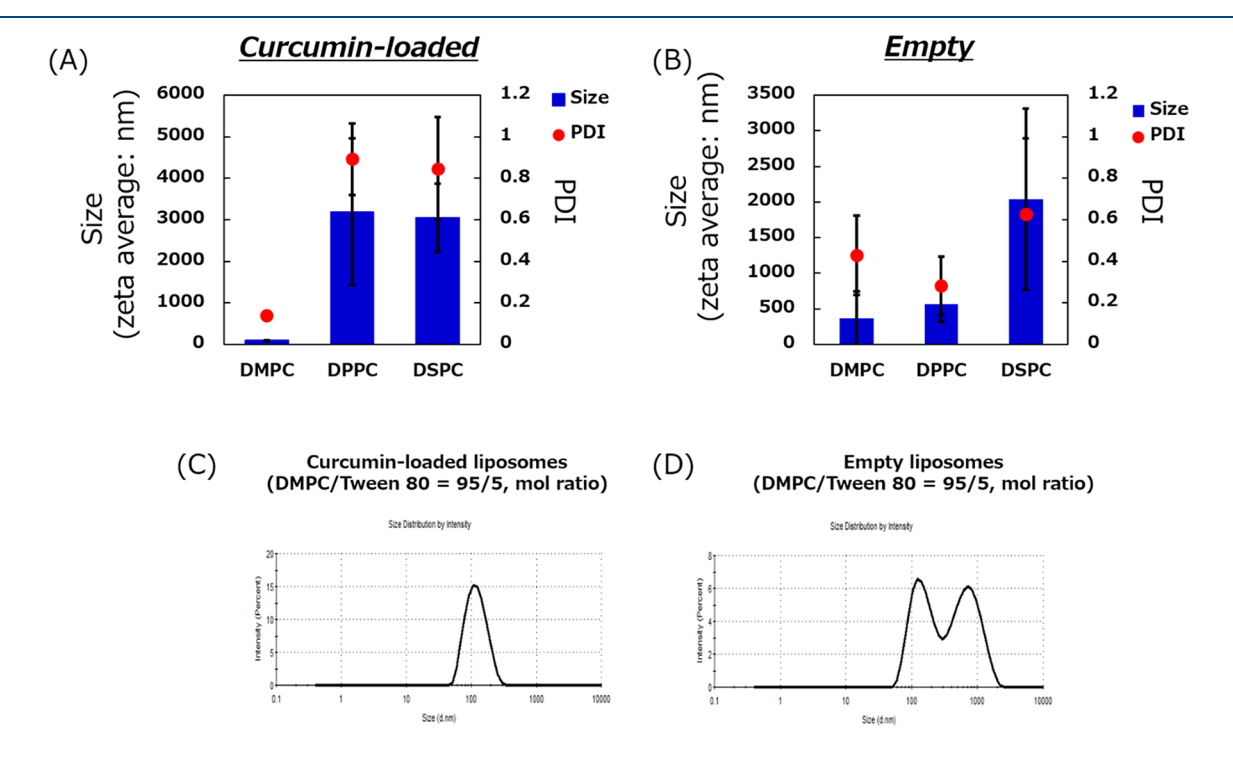


Figure 2. Effects of the acyl chain length of PC and curcumin on the average size, PDI, and size distribution of the resulting nanoparticles. Average size and PDI of different liposomal formulations with (A) or without (B) curcumin. Data = mean \pm SD (n = 3). Size distribution profiles of DMPC/Tween 80 (95/5) liposomes with (C) or without (D) curcumin.

curcumin in nanoparticles (~120 nm) with a narrow size distribution. Interestingly, when empty liposomes were prepared using the composition of PC/Tween 80 (95:5, mol), all three formulations displayed a large size (300-2000 nm with a high PDI of >0.3, Figure 2B). In particular, curcumin-containing liposomes composed of DMPC/Tween 80 (95:5) displayed a mean diameter of 120 nm with a single peak size distribution, while the empty DMPC/Tween 80 liposomes exhibited a larger size (~300 nm) with multiple peaks in the size distribution profile (Figure 2C,D). The data suggest that curcumin could interact with the DMPC/Tween 80 bilayer and stabilize the formulation to yield drugcontaining particles with a decreased size and improved uniformity. On the other hand, when curcumin was loaded within the DPPC/Tween 80 composition, the formulation aggregation was promoted (i.e., size increased from ~500 nm to 3000 nm). The DSPC/Tween 80 particles with or without curcumin displayed large aggregates (>2000 nm). It was reported previously that curcumin affected the function of membrane proteins by modifying the thickness and the elastic property of the host lipid bilayer³⁵ and acting like cholesterol with a significant impact on the membrane stability. 36,37 The study performed by Ali et al.³⁸ demonstrated that the lipid bilayer composed of a longer chain phospholipid displayed increased packing due to the enhanced interaction between the long acyl chains compared to the bilayer prepared with a shorter chain lipid. In other words, liposomal bilayer consisting of DMPC would exhibit increased flexibility to accommodate curcumin compared to that composed of DPPC or DSPC, and the increased curcumin-DMPC interaction led to a stabilized

3.1.3. Microfluidic Conditions. We then pursued to optimize the microfluidic conditions to produce optimal curcumin nanoparticles using the DMPC/Tween 80 formulation. We conducted studies investigating the effect of changing the total flow rate and flow ratio on the physical characteristics (size and PDI) of the prepared liposomal curcumin. We tested three different total flow rates, 17 mL/ min, 11 mL/min, and 5 mL/min, and three flow ratios (solvent/aqueous), 1:5, 1:3, and 1:1. It is noted that the D/L ratio and the final drug concentrations were fixed for each run. As shown in Table 2, regardless of the total flow rate, when the ratio of organic (ethanol) to aqueous (PBS) phase was decreased (from 1:1 to 1:3 to 1:5), both size and PDI of the resulting formulations decreased. At the highest flow ratio (1:1), the liposomal size ranged between 532 and 767 nm, and the PDI was >0.65. When the flow ratio was decreased to 1:3,

Table 2. Effects of Flow Rate Ratio and Total Flow Rate on Size and PDI of Liposomal Curcumin^a

flow rate	solvent to aqueous ratio	size (nm)	PDI
5 mL/min	1:1	532.2 ± 158.6	0.670 ± 0.09
	1:3	216.6 ± 23.5	0.230 ± 0.04
	1:5	126.9 ± 13.0	0.076 ± 0.03
11 mL/min	1:1	767.7 ± 277.6	0.680 ± 0.10
	1:3	241.1 ± 52.8	0.270 ± 0.05
	1:5	129.2 ± 4.4	0.126 ± 0.03
$17~\mathrm{mL/min}$	1:1	687.8 ± 201.7	0.664 ± 0.10
	1:3	219.7 ± 5.6	0.234 ± 0.02
	1:5	124.7 ± 4.2	0.100 ± 0.02

^aData = mean \pm SD, n = 3.

the particle size decreased to approximately 220 nm with a PDI of ~0.25. A final decrease of the flow ratio to 1:5 yielded even smaller liposomes with a mean diameter of ~125 nm and a PDI of \sim 0.1. The total flow rate, on the other hand, was not a critical parameter determining the particle size and PDI. The results were consistent with the previous reports. 23,24 At a high organic to aqueous ratio (1:1), the final ethanol concentration in the liposomal product was high (50%). Liposomes might not be properly formed in the presence of such a high concentration of ethanol and therefore displayed significant aggregation after dialysis. In contrast, at a low ratio of organic to aqueous flow (1:5), the amount of the organic solvent in the mixture was reduced to <20%, which allowed improved hydrophobic interaction among the lipids to form liposomes with enhanced stability. From the above data, we concluded that the optimal flow ratio was 1:5 (organic/water). Since a high total flow rate increased the efficiency of particle production, we then produced the optimized liposomal curcumin formulation (Lipo-Cur) under the following conditions: total flow rate 17 mL/min; flow ratio 1:5; formulation DMPC/Tween 80, 95:5.

3.1.4. Microfluidics versus Thin-Film Hydration. We also compared Lipo-Cur prepared with the microfluidic technology and the traditional thin-film hydration method. Although the products fabricated with these two techniques were comparable in size and PDI in the beginning, Lipo-Cur produced using the thin-film hydration method started to aggregate 1 day after storage at 4 °C, while that prepared with the microfluidics remained stable for 3 weeks (Figure 3). The data suggest that the preparation method affected curcumin and Tween 80 interaction with DMPC during bilayer formation, which influenced the product stability. During the microfluidic process, rapid mixing of the lipid/ethanol solution with the aqueous buffer resulted in a rapid increase in the polarity of the medium, which caused the solution to quickly achieve a state of high supersaturation of both curcumin and lipid monomers throughout the entire mixing volume,³⁹ leading to rapid and homogeneous nucleation of nanoparticles. It had been reported that these nucleation events were much faster compared to the time-scale for particle formation/aggregation. 39,40 Therefore, it is suggested that by using microfluidics, curcumin and DMPC could bind more rapidly and efficiently, which in turn might help distribute curcumin within the lipid bilayer more homogeneously. It is understood that small hydrophobic molecules like curcumin can occupy space left by defects in the packing of DMPC, leading to improved stability. Tween 80, being the most soluble component in the polar environment, experiences a lower driving force to assemble with the nascent liposome. Hence, we postulate that DMPC and curcumin are readily available to form the core of the nascent bilayer, and Tween 80 intercalates later and thus interacts mostly with the surface of the bilayer. On the other hand, in the case of thin film hydration, all of the components are well mixed in a low polarity environment prior to lipid cake formation, which allows more homogeneous distribution of Tween 80 among the other components. In this case, there is a greater opportunity for interaction between Tween 80 and curcumin, which could compete with curcumin-DMPC interactions that play an important role in bilayer stability. Additionally, during the microfluidic processes, the temperature was never raised above the phase transition temperature of DMPC (24 °C) so that Tween 80 at the surface would have a limited opportunity to diffuse into the bilayer where it could

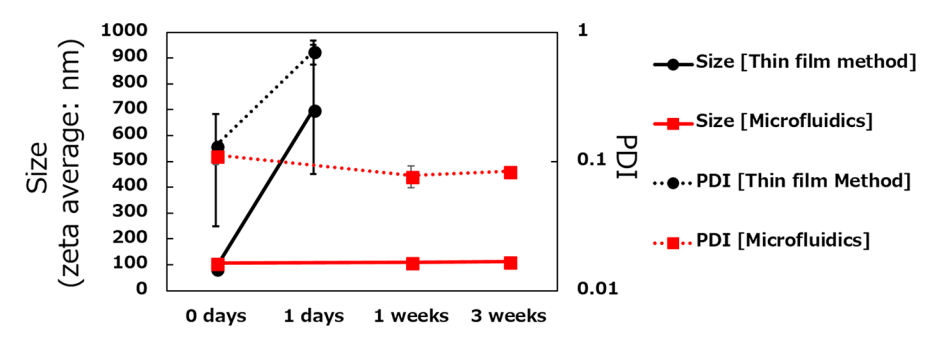


Figure 3. Stability of Lipo-Cur prepared by the thin-film method and the microfluidics after storage at 4 °C. Data = mean \pm SD (n = 3).

Table 3. Summary of Formulation Parameters of Lipo-Cur^a

lipid nanoparticles	size	PDI	curcumin concentration $(\mu \mathrm{g/mL})$	dose recovery for curcumin (%)	estimated loading capacity (%)
Lipo-Cur [DMPC/Tween 80 = 95:5 (mol)]	116.4 ± 5.5	0.140 ± 0.025	278.7 ± 40.4	87.7 ± 10.7	17.1 ± 2.1
^a Data = mean \pm SD, $n = 3-5$.					

compete with DMPC in interacting with curcumin. To the best of our knowledge, this was the first example of using microfluidics to prepare a liposomal formulation for curcumin. Microfluidics has only been employed to formulate curcumin in PLGA nanoparticles $^{41,42}_{}$ and to fabricate liposomes for the delivery of other drugs. $^{23-25}_{}$

3.2. Characterization of Optimal Lipo-Cur. As shown in Table 3, the optimal Lipo-Cur prepared with the microfluidics exhibited a size of 116.4 ± 5.48 nm with a narrow PDI (<0.15). The dose recovery for curcumin using this liposomal formulation was 87.7 \pm 10.7%, the estimated D/L was approximately 1:5.85, and the estimated loading capacity was around 17 wt % (Table 3). Also, Lipo-Cur formulation increased the water solubility of curcumin by ~700-fold (Table 3). As the D/L was impressively high for a hydrophobic drug passively loaded into liposomes, we first questioned whether Lipo-Cur was indeed in the liposomal conformation. Therefore, Lipo-Cur morphology was examined using cryo-TEM. As shown in Figure 4, Lipo-Cur displayed a standard small unilamellar vesicular structure of liposomes. It has been reported by many groups that the loading capacity of a typical liposomal formulation for a wide range of hydrophobic drugs is

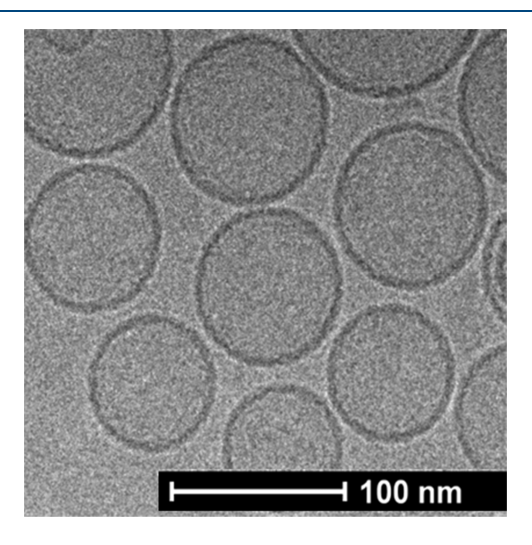


Figure 4. Representative cryo-TEM image of Lipo-Cur.

normally <5 wt %. 17,18,43 With the data support from Figure 2 and the earlier discussion in Section 3.1.2, it is speculated that curcumin could be incorporated between the lipids in the DMPC/Tween 80 membrane, achieving high drug loading and stabilizing the liposomal formulation, similar functions as cholesterol in standard liposomal formulations. 44 In fact, the D/L achieved by other liposomal curcumin formulations was between 0.025 and 0.04 (w/w), 17,18 and to the best of our knowledge, our Lipo-Cur formulation provided the highest D/L (1:5.85 = 0.17 wt/wt). To deliver a fixed drug dose, a liposomal formulation with an increased D/L allows administrating a reduced dose of lipid excipients. The advantages include significant saving on the lipids when manufacturing the formulation and decreased concern of side effects from the lipid excipients.

The drug release study of Lipo-Cur was performed in serum and displayed a rapid release profile (Figure 5). After 4 h,

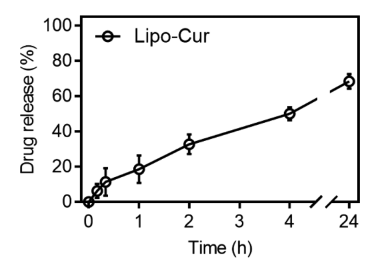


Figure 5. In vitro drug release from Lipo-Cur in 50% FBS at 37 °C. Data = mean \pm SD (n = 3).

approximately 50% of curcumin was released. Hydrophobic drugs passively loaded inside the hydrophobic compartment of nanoparticles have been shown to rapidly release in the presence of serum. The data suggest again that curcumin was loaded in the lipid bilayer of Lipo-Cur.

3.3. In Vivo Results. 3.3.1. Pharmacokinetics (PK). Curcumin has been shown to regulate a few transcription factors in cells such as STAT3, NF- κ B, and PPAR- γ . When incubated with tumor cells, curcumin inhibits STAT3 and NF- κ B, and upregulates PPAR- γ , ^{12,15,49,50} resulting in antiangiogenesis, cellular apoptosis, and sensitization of tumor cells to chemotherapy. ^{12,15,51} Recently, it was reported that curcumin

suppressed regulatory T cells and significantly increased Th1 (helper T cell) response. Because of these mechanisms, curcumin has been investigated as an anticancer drug. However, its clinical application has been hampered by poor solubility.

Curcumin is mainly formulated in an aqueous suspension or dissolved in oil for oral or i.p. administration for animal studies. ^{11,15,30} As curcumin is water-insoluble, the absorption of these standard formulations is poor, requiring frequent administrations of a large dose to exert in vivo efficacy. Lipo-Cur dispersed curcumin in nanosized particles, increasing the water solubility from 0.4 to ~280 μ g/mL, which enabled both i.v. and oral delivery with significant potential to increase the drug exposure. To test whether Lipo-Cur displayed increased drug exposure relative to the standard formulation, we first examined the PK of i.v. and oral Lipo-Cur in comparison with an oral curcumin suspension in mice. As shown in Figure 6 and

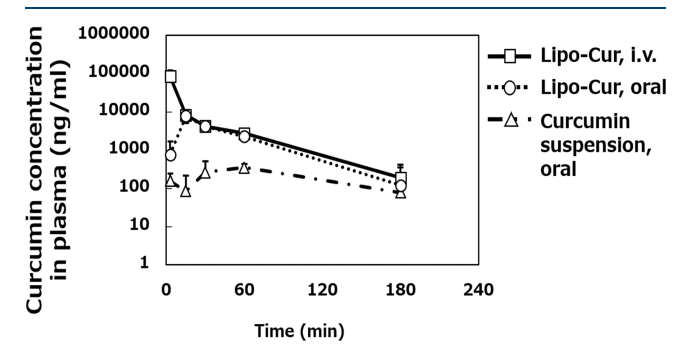


Figure 6. Pharmacokinetics of curcumin formulations in female C57BL6 mice. Dose = 20 mg curcumin/kg. Data = mean \pm SD (n = 3).

Table 4, the oral curcumin suspension was poorly absorbed with low plasma concentrations (100-350 ng/mL) for the first 3 h after dosing, and the C_{max} at 251 ng/mL was detected at 1 h post oral delivery, which indicated inefficient and slow absorption. On the other hand, Lipo-Cur was rapidly absorbed, achieving a > 10-fold higher C_{max} (4160 ng/mL) at 0.5 h post oral delivery. The area under the curve (AUC) of oral Lipo-Cur was 7.8-fold higher than that of the oral curcumin suspension, and the oral bioavailability of these two formulations was approximately 40% and 5%, respectively. The results indicate that Lipo-Cur was better absorbed orally compared to the curcumin suspension, possibly due to increased water solubility. Because Lipo-Cur was a waterbased formulation, it could also be intravenously delivered. As shown in Figure 6, i.v. Lipo-Cur produced a high plasma concentration right after injection (84 676 ng/mL), and the plasma profile reached the elimination phase in 0.5 h with a half-life of 33 min. It is noted that the elimination phase of the plasma profile of i.v. Lipo-Cur overlapped with that of oral Lipo-Cur, which indicated the same elimination half-life for both routes. The data suggest that the liposomal formulation

served as a solubilizing vehicle for curcumin and had only minor influence on the PK. The PK data of Lipo-Cur are consistent with its rapid drug release profile in serum (Figure 5).

The PK data demonstrated that Lipo-Cur was a flexible formulation that could be delivered by oral and i.v. with increased drug exposure compared to the standard curcumin suspension. We then selected the i.v. route for Lipo-Cur for the following animal studies to ensure complete systemic bioavailability.

3.3.2. Anticancer Efficacy and Safety. We evaluated the antitumor activity of Lipo-Cur in two s.c. syngeneic tumor models in mice. EMT6 murine breast tumor and B16F10 murine melanoma cells were s.c. inoculated into BALB/c and C57BL/6 mice, respectively. After 7 to 10 days post tumor inoculation, the mice were randomly assigned to receive an injection of either saline, free cisplatin (CDDP), Lipo-Cur, or combination of CDDP and Lipo-Cur. The efficacy results were comparable in both models that Lipo-Cur and CDDP exhibited significant and similar antitumor efficacy, and the combination treatment displayed further enhanced effect (Figure 7). In the EMT6 model, Lipo-Cur, CDDP, and combination inhibited the tumor growth by 39, 46, and 77% on day 6 relative to the control, respectively (Figure 7B). The antitumor effect was even more significant in the B16F10 model, wherein Lipo-Cur, CDDP, and combination inhibited the tumor growth on day 6 by 46, 63, and 74% relative to the control, respectively (Figure 7B). The data suggest Lipo-Cur formulation when used alone was as effective as CDDP in inhibiting the tumor growth and augmented CDDP efficacy when used in combination.

During this efficacy study, one BALB/C mouse in the CDDP group reached a humane end point 3 days after treatment, while all mice in the combination group survived. While CDDP has been shown effective in treating a wide range of cancers, 54,55 its clinical efficacy has been hampered by significant side effects including nephrotoxicity, ototoxicity, and neurotoxicity. Among these adverse effects, nephrotoxicity limits the CDDP dose that can be safely given to human patients. It has been reported that i.p. delivered CDDP at 15 mg/kg induced evident kidney toxicity in BALB/C mice 3 days after the drug administration. 56,57 It was speculated that the mouse reached the end point in the CDDP group due to significant nephrotoxicity, and our data suggest that Lipo-Cur might reduce the nephrotoxicity induced by CDDP. Therefore, we further examined the protective effect of Lipo-Cur against CDDP-induced kidney toxicity. The kidneys and serum were isolated from BALB/C mice 3 days after treatment with either saline, Lipo-Cur, CDDP, or combination of Lipo-Cur and CDDP. The kidney histology and serum BUN level were determined to investigate the kidney damage in each group. As shown in Figure 8A, CDDP induced significant acute tubular necrosis, and multiple necrotic cells and debris in the tubule lumen were indicated by the arrows, while the kidney histology

Table 4. Pharmacokinetic Parameters of Lip-Cur and Curcumin Suspension Given by i.v. or Oral^a

	$C_{\text{max}} (\text{ng/mL})$	AUC (min μ g/mL)	$T_{ m max}$ (min)	bioavailability (%)
Lipo-Cur [i.v.]	84676 ± 35232	1023.7 ± 143.8	1	100.0
Lipo-Cur [Oral]	4160 ± 962	401.4 ± 110.3	30	39.2 ± 10.2
curcumin suspension [Oral]	351 ± 86	51.4 ± 22.0	60	5.0 ± 1.8

^aData = mean \pm SD, n = 3.

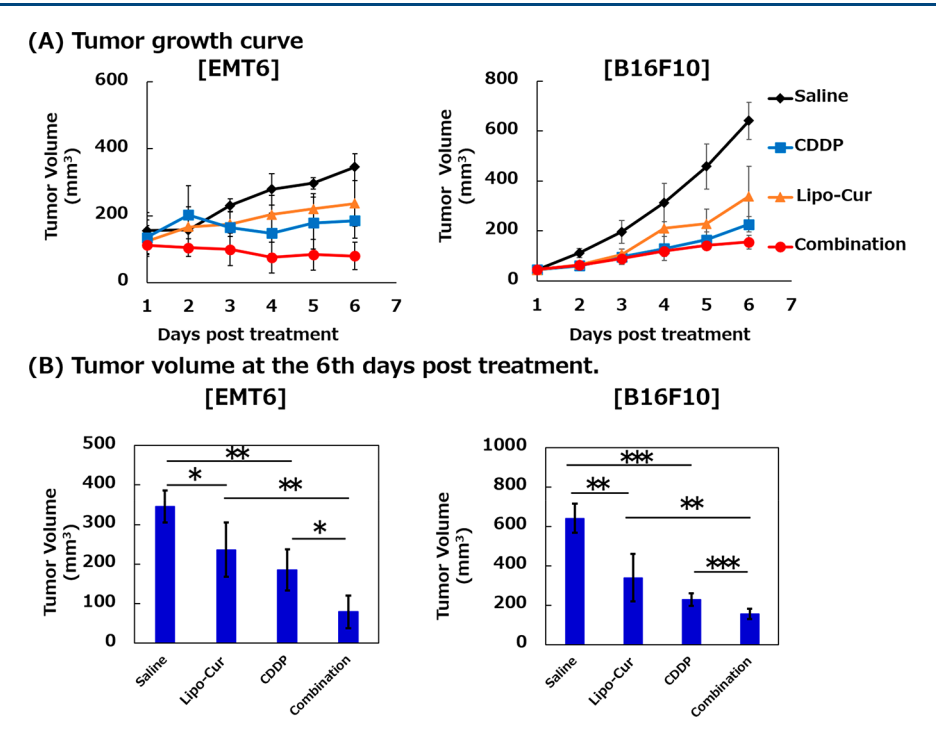


Figure 7. In vivo efficacy of different treatments against EMT-6 and B16F10 tumor models. Tumor growth kinetics (A) and tumor volume (B) on day 6. Tumor-bearing mice were injected with saline, Lipo-Cur (20 mg/kg), cisplatin (CDDP: 15 mg/kg), or combination (Lipo-Cur + CDDP) on day 0. Data = mean \pm SD (n = 5). **p < 0.05, ***p < 0.01, ***p < 0.005.

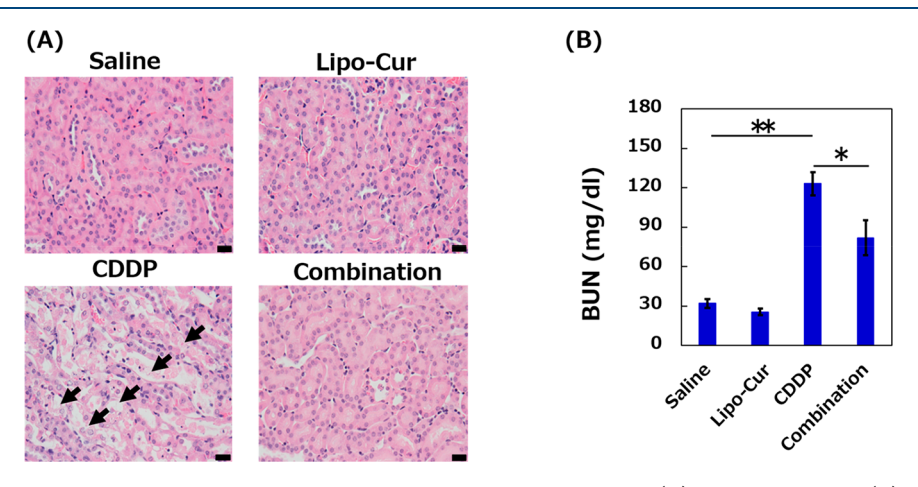


Figure 8. Effect of Lipo-Cur on cisplatin-induced renal tubular damage. HE staining of kidneys (A). Serum BUN level (B). Mice were injected with saline, Lipo-Cur (20 mg/kg), CDDP (15 mg/kg), or combination (Lipo-Cur + CDDP). After 3 days, kidney and serum were collected for analyses (data = mean \pm S.D, n = 3). Arrows show tubular necrosis, and the scale represents 20 μ m. *p < 0.05.

was normal in other groups. Serum BUN is an early marker of kidney toxicity,⁵⁸ and the level was elevated by four-fold after CDDP therapy compared to the saline control and Lipo-Cur (Figure 8B). When CDDP was used in combination with Lipo-Cur, the serum BUN level was significantly reduced from 120 mg/dL to 80 mg/dL, which suggested reduced kidney toxicity.

Together, our efficacy and safety data indicated that Lipo-Cur given at a single and low dose exhibited significant anticancer effect when used alone, and augmented the efficacy and suppressed the dose-limiting side effect of CDDP when used in combination. In previous reports, curcumin needed to be premedicated at high and frequent doses before CDDP to enhance the efficacy and reduce the side effects. Lis,59 Kumar et al. orally delivered a curcumin suspension at 120 mg/kg/day for 5 consecutive days before an i.p. dose of CDDP at 7.5 mg/

kg to rats bearing breast cancer. The tumor growth inhibition by curcumin alone, CDDP alone, and the combination was 20%, 24%, and 66%, respectively. The intensive pretreatment with curcumin also reduced nephrotoxicity of CDDP. In another study, curcumin (200 mg/kg) was orally given to rats 30 min before and 24 and 48 h after CDDP therapy at 5 mg/kg to effectively ameliorate the kidney toxicity of CDDP. To the best of our knowledge, our work disclosed the first curcumin formulation that enhanced antitumor efficacy and reduced toxicity of CDDP simultaneously under a single and low dose of curcumin that was coadministered with CDDP. This significant enhancement in efficacy is likely due to the improved systemic exposure of Lipo-Cur as shown in Figure 6 and Table 4. If translated to the clinical setting, Lipo-Cur may provide several advantages to improve current CDDP

therapy compared to the previously reported curcumin formulations. First, the single dose and coadministration dosing regimen is convenient, promoting patient compliance. Second, CDDP and curcumin can be coadministered without delaying CDDP therapy. Third, both the efficacy and safety of the therapy will be enhanced. At present, the underlying mechanism that curcumin suppressed the CDDP-induced kidney toxicity remains unknown. It was shown that CDDP activated NF-κB, a transcriptional factor driving the proinflammatory pathway in the kidneys, therefore, NF-κB could be the major target for curcumin to exert its antitumor/chemosensitizing activity and chemo-protection effect in the tumor and kidney, respectively.

4. CONCLUSION

A liposomal curcumin formulation (Lipo-Cur) was developed and fabricated using robust microfluidics. Both the lipid formulation and microfluidic parameters were optimized to produce Lipo-Cur with desirable physical properties, drug loading efficiency, and stability. Lipo-Cur exhibited a size of ~120 nm and a uniformed size distribution profile, provided high loading capacity for curcumin (~17 wt %), and a 700-fold increase in water solubility, leading to 8–20-fold increased AUC for the PK profile relative to the standard oral curcumin suspension. When coinjected with CDDP at a relatively low dose, the antitumor efficacy and safety of CDDP were both enhanced by Lipo-Cur. The results suggest significant potential of Lipo-Cur for improving CDDP therapy.

AUTHOR INFORMATION

Corresponding Author

*E-mail: shyh-dar.li@ubc.ca. Phone: 604-827-0675. Fax: 604-822-3035.

ORCID ®

Jayesh A. Kulkarni: 0000-0002-3622-6998 Pieter R. Cullis: 0000-0001-9586-2508 Shyh-Dar Li: 0000-0002-1763-2667

Notes

The authors declare the following competing financial interest(s): One of the authors, Shell Ip, is employed by Precision Nanosystems Inc. that manufactures the microfluidic device for making Lipo-Cur.

The data that support the plots within this paper and other findings of this study are available from the corresponding author upon reasonable request.

ACKNOWLEDGMENTS

This research was supported by grants from Canadian Institutes of Health Research (CIHR), Natural Sciences and Engineering Research Council of Canada, and Canada Foundation of Innovation. N.H. was supported by the Uehara Memorial Foundation Research Fellowship. S.-D.L. is a recipient of CIHR New Investigator Salary Awards and the Angiotech Professorship in Drug Delivery.

REFERENCES

- (1) Srimal, R. C.; Dhawan, B. N. Pharmacology of Diferuloyl Methane (Curcumin), a Non-Steroidal Anti-Inflammatory Agent. *J. Pharm. Pharmacol.* **1973**, *25* (6), 447–452.
- (2) Satoskar, R. R.; Shah, S. J.; Shenoy, S. G. Evaluation of Anti-Inflammatory Property of Curcumin (Diferuloyl Methane) in Patients

with Postoperative Inflammation. *Int. J. Clin. Pharmacol. Ther. Toxicol.* **1986**, 24 (12), 651–654.

- (3) Kuttan, R.; Bhanumathy, P.; Nirmala, K.; George, M. C. Potential Anticancer Activity of Turmeric (Curcuma Longa). *Cancer Lett.* **1985**, *29* (2), 197–202.
- (4) Sharma, O. P. Antioxidant Activity of Curcumin and Related Compounds. *Biochem. Pharmacol.* 1976, 25 (15), 1811–1812.
- (5) Toda, S.; Miyase, T.; Arichi, H.; Tanizawa, H.; Takino, Y. Natural Antioxidants. III. Antioxidative Components Isolated from Rhizome of Curcuma Longa L. Chem. Pharm. Bull. 1985, 33 (4), 1725–1728.
- (6) Sidhu, G. S.; Singh, a K.; Thaloor, D.; Banaudha, K. K.; Patnaik, G. K.; Srimal, R. C.; Maheshwari, R. K. Enhancement of Wound Healing by Curcumin in Animals. *Wound Repair Regen.* 1998, 6 (2), 167–177.
- (7) Negi, P. S.; Jayaprakasha, G. K.; Rao, L. J. M.; Sakariah, K. K. Antibacterial Activity of Turmeric Oil: A Byproduct from Curcumin Manufacture. *J. Agric. Food Chem.* **1999**, *47* (10), 4297–4300.
- (8) CFR Code of Federal Regulations Title 21; U.S. FDA, 2018.
- (9) Notarbartolo, M.; Poma, P.; Perri, D.; Dusonchet, L.; Cervello, M.; D'Alessandro, N. Antitumor Effects of Curcumin, Alone or in Combination with Cisplatin or Doxorubicin, on Human Hepatic Cancer Cells. Analysis of Their Possible Relationship to Changes in NF-KB Activation Levels and in IAP Gene Expression. *Cancer Lett.* **2005**, *224* (1), 53–65.
- (10) Selvendiran, K.; Ahmed, S.; Dayton, A.; Kuppusamy, M. L.; Rivera, B. K.; Kálai, T.; Hideg, K.; Kuppusamy, P. HO-3867, a Curcumin Analog, Sensitizes Cisplatin-Resistant Ovarian Carcinoma, Leading to Therapeutic Synergy through STAT3 Inhibition. *Cancer Biol. Ther.* **2011**, *12* (9), 837–845.
- (11) Ueki, M.; Ueno, M.; Morishita, J.; Maekawa, N. Curcumin Ameliorates Cisplatin-Induced Nephrotoxicity by Inhibiting Renal Inflammation in Mice. *J. Biosci. Bioeng.* **2013**, *115* (5), 547–551.
- (12) Fetoni, A. R.; Paciello, F.; Mezzogori, D.; Rolesi, R.; Eramo, S. L. M.; Paludetti, G.; Troiani, D. Molecular Targets for Anticancer Redox Chemotherapy and Cisplatin-Induced Ototoxicity: The Role of Curcumin on PSTAT3 and Nrf-2 Signalling. *Br. J. Cancer* **2015**, *113*, 1434–1444
- (13) Kumari, P.; Swami, M. O.; Nadipalli, S. K.; Myneni, S.; Ghosh, B.; Biswas, S. Curcumin Delivery by Poly(Lactide)-Based Co-Polymeric Micelles: An In Vitro Anticancer Study. *Pharm. Res.* **2016**, 33 (4), 826–841.
- (14) Shahani, K.; Swaminathan, S. K.; Freeman, D.; Blum, A.; Ma, L.; Panyam, J. Injectable Sustained Release Microparticles of Curcumin: A New Concept for Cancer Chemoprevention. *Cancer Res.* **2010**, *70* (11), 4443–4452.
- (15) Kumar, P.; Barua, C. C.; Sulakhiya, K.; Sharma, R. K. Curcumin Ameliorates Cisplatin-Induced Nephrotoxicity and Potentiates Its Anticancer Activity in SD Rats: Potential Role of Curcumin in Breast Cancer Chemotherapy. *Front. Pharmacol.* **2017**, 8 (APR), 1.
- (16) Yallapu, M. M.; Jaggi, M.; Chauhan, S. C. Curcumin Nanoformulations: A Future Nanomedicine for Cancer. *Drug Discovery Today* **2012**, *17* (1–2), 71–80.
- (17) Pamunuwa, G.; Karunaratne, V.; Karunaratne, D. N. Effect of Lipid Composition on *In Vitro* Release and Skin Deposition of Curcumin Encapsulated Liposomes. *J. Nanomater.* **2016**, 2016, 1–9.
- (18) Saengkrit, N.; Saesoo, S.; Srinuanchai, W.; Phunpee, S.; Ruktanonchai, U. R. Influence of Curcumin-Loaded Cationic Liposome on Anticancer Activity for Cervical Cancer Therapy. *Colloids Surf., B* **2014**, *114*, 349–356.
- (19) Sari, T. P.; Mann, B.; Kumar, R.; Singh, R. R. B.; Sharma, R.; Bhardwaj, M.; Athira, S. Preparation and Characterization of Nanoemulsion Encapsulating Curcumin. *Food Hydrocolloids* **2015**, 43, 540–546.
- (20) Gou, M.; Men, K.; Shi, H.; Xiang, M.; Zhang, J.; Song, J.; Long, J.; Wan, Y.; Luo, F.; Zhao, X.; et al. Curcumin-Loaded Biodegradable Polymeric Micelles for Colon Cancer Therapy in Vitro and in Vivo. *Nanoscale* **2011**, *3* (4), 1558.

(21) Yu, Y.; Zhang, X.; Qiu, L. The Anti-Tumor Efficacy of Curcumin When Delivered by Size/Charge-Changing Multistage Polymeric Micelles Based on Amphiphilic Poly(β -Amino Ester) Derivates. *Biomaterials* **2014**, 35 (10), 3467–3479.

- (22) Zhang, J.; Li, J.; Shi, Z.; Yang, Y.; Xie, X.; Lee, S. M.; Wang, Y.; Leong, K. W.; Chen, M. PH-Sensitive Polymeric Nanoparticles for Co-Delivery of Doxorubicin and Curcumin to Treat Cancer via Enhanced pro-Apoptotic and Anti-Angiogenic Activities. *Acta Biomater.* **2017**, *58*, 349–364.
- (23) Kastner, E.; Verma, V.; Lowry, D.; Perrie, Y. Microfluidic-Controlled Manufacture of Liposomes for the Solubilisation of a Poorly Water Soluble Drug. *Int. J. Pharm.* **2015**, *485* (1–2), 122–130.
- (24) Joshi, S.; Hussain, M. T.; Roces, C. B.; Anderluzzi, G.; Kastner, E.; Salmaso, S.; Kirby, D. J.; Perrie, Y. Microfluidics Based Manufacture of Liposomes Simultaneously Entrapping Hydrophilic and Lipophilic Drugs. *Int. J. Pharm.* **2016**, *514* (1), 160–168.
- (25) Carugo, D.; Bottaro, E.; Owen, J.; Stride, E.; Nastruzzi, C. Liposome Production by Microfluidics: Potential and Limiting Factors. Sci. Rep. 2016, 6 (1), 25876.
- (26) Hood, R. R.; DeVoe, D. L. High-Throughput Continuous Flow Production of Nanoscale Liposomes by Microfluidic Vertical Flow Focusing. *Small* **2015**, *11* (43), 5790–5799.
- (27) Ran, R.; Middelberg, A. P. J.; Zhao, C.-X. Microfluidic Synthesis of Multifunctional Liposomes for Tumour Targeting. *Colloids Surf.*, B **2016**, *148*, 402–410.
- (28) Kulkarni, J. A.; Tam, Y. Y. C.; Chen, S.; Tam, Y. K.; Zaifman, J.; Cullis, P. R.; Biswas, S. Rapid Synthesis of Lipid Nanoparticles Containing Hydrophobic Inorganic Nanoparticles. *Nanoscale* **2017**, *9* (36), 13600–13609.
- (29) Mills, J. K.; Needham, D. Lysolipid Incorporation in Dipalmitoylphosphatidylcholine Bilayer Membranes Enhances the Ion Permeability and Drug Release Rates at the Membrane Phase Transition. *Biochim. Biophys. Acta, Biomembr.* **2005**, *1716* (2), 77–96.
- (30) Zhongfa, L.; Chiu, M.; Wang, J.; Chen, W.; Yen, W.; Fan-Havard, P.; Yee, L. D.; Chan, K. K. Enhancement of Curcumin Oral Absorption and Pharmacokinetics of Curcuminoids and Curcumin Metabolites in Mice. *Cancer Chemother. Pharmacol.* **2012**, *69* (3), 679–689.
- (31) Israelachvili, J. N.; Mitchell, D. J. A Model for the Packing of Lipids in Bilayer Membranes. *Biochim. Biophys. Acta, Biomembr.* **1975**, 389 (1), 13–19.
- (32) Israelachvili, J. N.; Mitchell, D. J.; Ninham, B. W. Theory of Self-Assembly of Lipid Bilayers and Vesicles. *Biochim. Biophys. Acta, Biomembr.* 1977, 470 (2), 185–201.
- (33) Stuart, M. C. A.; Boekema, E. J. Two Distinct Mechanisms of Vesicle-to-Micelle and Micelle-to-Vesicle Transition Are Mediated by the Packing Parameter of Phospholipid—Detergent Systems. *Biochim. Biophys. Acta, Biomembr.* **2007**, *1768* (11), 2681–2689.
- (34) Dennis, E. A. Micellization and Solubilization of Phospholipids by Surfactants. *Adv. Colloid Interface Sci.* **1986**, *26*, 155–175.
- (35) Hung, W.-C.; Chen, F.-Y.; Lee, C.-C.; Sun, Y.; Lee, M.-T.; Huang, H. W. Membrane-Thinning Effect of Curcumin. *Biophys. J.* **2008**, *94* (11), 4331–4338.
- (36) Semple, S. C.; Chonn, A.; Cullis, P. R. Influence of Cholesterol on the Association of Plasma Proteins with Liposomes. *Biochemistry* **1996**, 35 (8), 2521–2525.
- (37) Karewicz, A.; Bielska, D.; Gzyl-Malcher, B.; Kepczynski, M.; Lach, R.; Nowakowska, M. Interaction of Curcumin with Lipid Monolayers and Liposomal Bilayers. *Colloids Surf., B* **2011**, 88 (1), 231–239.
- (38) Ali, M. H.; Moghaddam, B.; Kirby, D. J.; Mohammed, A. R.; Perrie, Y. The Role of Lipid Geometry in Designing Liposomes for the Solubilisation of Poorly Water Soluble Drugs. *Int. J. Pharm.* **2013**, 453 (1), 225–232.
- (39) Belliveau, N. M.; Huft, J.; Lin, P. J.; Chen, S.; Leung, A. K.; Leaver, T. J.; Wild, A. W.; Lee, J. B.; Taylor, R. J.; Tam, Y. K.; et al. Microfluidic Synthesis of Highly Potent Limit-Size Lipid Nanoparticles for In Vivo Delivery of SiRNA. *Mol. Ther.–Nucleic Acids* **2012**, *1*, e37.

- (40) Zhigaltsev, I. V.; Belliveau, N.; Hafez, I.; Leung, A. K. K.; Huft, J.; Hansen, C.; Cullis, P. R. Bottom-Up Design and Synthesis of Limit Size Lipid Nanoparticle Systems with Aqueous and Triglyceride Cores Using Millisecond Microfluidic Mixing. *Langmuir* **2012**, 28 (7), 3633–3640.
- (41) Gdowski, A.; Johnson, K.; Shah, S.; Gryczynski, I.; Vishwanatha, J.; Ranjan, A. Optimization and Scale up of Microfluidic Nanolipomer Production Method for Preclinical and Potential Clinical Trials. *J. Nanobiotechnol.* **2018**, *16* (1), 12.
- (42) Morikawa, Y.; Tagami, T.; Hoshikawa, A.; Ozeki, T. The Use of an Efficient Microfluidic Mixing System for Generating Stabilized Polymeric Nanoparticles for Controlled Drug Release. *Biol. Pharm. Bull.* **2018**, *41* (6), 899–907.
- (43) Mahmud, M.; Piwoni, A.; Filiczak, N.; Janicka, M.; Gubernator, J. Long-Circulating Curcumin-Loaded Liposome Formulations with High Incorporation Efficiency, Stability and Anticancer Activity towards Pancreatic Adenocarcinoma Cell Lines In Vitro. *PLoS One* **2016**, *11* (12), e0167787.
- (44) Briuglia, M.-L.; Rotella, C.; McFarlane, A.; Lamprou, D. A. Influence of Cholesterol on Liposome Stability and on in Vitro Drug Release. *Drug Delivery Transl. Res.* **2015**, *5* (3), 231–242.
- (45) Chountoulesi, M.; Naziris, N.; Pippa, N.; Demetzos, C. The Significance of Drug-to-Lipid Ratio to the Development of Optimized Liposomal Formulation. *J. Liposome Res.* **2018**, *6*, 1–10.
- (46) Xu, Q.; Tanaka, Y.; Czernuszka, J. T. Encapsulation and Release of a Hydrophobic Drug from Hydroxyapatite Coated Liposomes. *Biomaterials* **2007**, 28 (16), 2687–2694.
- (47) Kan, P.; Tsao, C.-W.; Wang, A.-J.; Su, W.-C.; Liang, H.-F. A Liposomal Formulation Able to Incorporate a High Content of Paclitaxel and Exert Promising Anticancer Effect. *J. Drug Delivery* **2011**, 2011, 629234.
- (48) Zhou, H.; Beevers, C. S.; Huang, S. The Targets of Curcumin. Curr. Drug Targets 2011, 12 (3), 332–347.
- (49) Mazidi, M.; Karimi, E.; Meydani, M.; Ghayour-Mobarhan, M.; Ferns, G. A. Potential Effects of Curcumin on Peroxisome Proliferator-Activated Receptor-γ in Vitro and in Vivo. *World J. Methodol.* **2016**, *6* (1), 112–117.
- (50) Joe, B.; Vijaykumar, M.; Lokesh, B. R. Biological Properties of Curcumin-Cellular and Molecular Mechanisms of Action. *Crit. Rev. Food Sci. Nutr.* **2004**, 44 (2), 97–111.
- (51) Maheshwari, R. K.; Singh, A. K.; Gaddipati, J.; Srimal, R. C. Multiple Biological Activities of Curcumin: A Short Review. *Life Sci.* **2006**, 78, 2081–2087.
- (52) Zou, J. Y.; Su, C. H.; Luo, H. H.; Lei, Y. Y.; Zeng, B.; Zhu, H. S.; Chen, Z. G. Curcumin Converts Foxp3+ Regulatory T Cells to T Helper 1 Cells in Patients with Lung Cancer. *J. Cell. Biochem.* **2018**, 119 (2), 1420–1428.
- (53) Xu, B.; Yu, L.; Zhao, L.-Z. Curcumin up Regulates T Helper 1 Cells in Patients with Colon Cancer. *Am. J. Transl. Res.* **2017**, 9 (4), 1866–1875.
- (54) Lebwohl, D.; Canetta, R. Clinical Oncology Update Clinical Development of Platinum Complexes in Cancer Therapy: An Historical Perspective and an Update. *Eur. J. Cancer* 1998, 34, 1522.
- (55) Florea, A.-M.; Busselberg, D. Cisplatin as an Anti-Tumor Drug: Cellular Mechanisms of Activity, Drug Resistance and Induced Side Effects. *Cancers* **2011**, *3*, 1351.
- (56) Mishima, K.; Baba, A.; Matsuo, M.; Itoh, Y.; Oishi, R. Protective Effect of Cyclic AMP against Cisplatin-Induced Nephrotoxicity. *Free Radical Biol. Med.* **2006**, 40 (9), 1564–1577.
- (57) Faubel, S.; Lewis, E. C.; Reznikov, L.; Ljubanovic, D.; Hoke, T. S.; Somerset, H.; Oh, D.-J.; Lu, L.; Klein, C. L.; Dinarello, C. A.; et al. Cisplatin-Induced Acute Renal Failure Is Associated with an Increase in the Cytokines Interleukin (IL)-1beta, IL-18, IL-6, and Neutrophil Infiltration in the Kidney. *J. Pharmacol. Exp. Ther.* **2007**, 322 (1), 8–15.
- (58) Gowda, S.; Desai, P. B.; Kulkarni, S. S.; Hull, V. V.; Math, A. A. K.; Vernekar, S. N. Markers of Renal Function Tests. N. Am. J. Med. Sci. **2010**, 2 (4), 170–173.

(59) Trujillo, J.; Molina-Jijón, E.; Medina-Campos, O. N.; Rodríguez-Muñoz, R.; Reyes, J. L.; Loredo, M. L.; Barrera-Oviedo, D.; Pinzón, E.; Rodríguez-Rangel, D. S.; Pedraza-Chaverri, J. Curcumin Prevents Cisplatin-Induced Decrease in the Tight and Adherens Junctions: Relation to Oxidative Stress. *Food Funct.* **2016**, 7 (1), 279–293.

- (60) Conte, P. F.; Bruzzone, M.; Carnino, F.; Gadducci, A.; Algeri, R.; Bellini, A.; Boccardo, F.; Brunetti, I.; Catsafados, E.; Chiara, S.; et al. High-Dose versus Low-Dose Cisplatin in Combination with Cyclophosphamide and Epidoxorubicin in Suboptimal Ovarian Cancer: A Randomized Study of the Gruppo Oncologico Nord-Ovest. J. Clin. Oncol. 1996, 14 (2), 351–356.
- (61) Szturz, P.; Wouters, K.; Kiyota, N.; Tahara, M.; Prabhash, K.; Noronha, V.; Castro, A.; Licitra, L.; Adelstein, D.; Vermorken, J. B. Weekly Low-Dose Versus Three-Weekly High-Dose Cisplatin for Concurrent Chemoradiation in Locoregionally Advanced Non-Nasopharyngeal Head and Neck Cancer: A Systematic Review and Meta-Analysis of Aggregate Data. *Oncologist* 2017, 22 (9), 1056—1066.